Power Allocation for FAS-assisted Downlink Communication

Boyi Tang*, Hao Xu*, Kai-Kit Wong*, Li You†, Wee Kiat New*, Jie Tang‡, and Xiu Yin Zhang‡
*Department of Electronic and Electrical Engineering, University College London, London WC1E7JE, U.K.
†National Mobile Communications Research Laboratory, Southeast University, Nanjing 210096, China
‡ School of Electronic and Information Engineering, South China University of Technology, Guangzhou 510640, China
E-mail: {boyi.tang.22, hao.xu, kai-kit.wong, a.new}@ucl.ac.uk; lyou@seu.edu.cn; {eejtang, zhangxiuyin}@scut.edu.cn

***Abstract*—Fluid antenna is a novel technology that can switch its radiating element to different locations within a predefined space. Utilizing the natural fading of the signal envelope, fluid antenna can select the best channel without complicated signal processing. This paper studies two power allocation problems in a downlink multi-user fluid antenna system (FAS), where each user is equipped with a fluid antenna while the base station (BS) has multiple fixed-position antennas (FPAs). We first aim to minimize the total transmit power of the BS with quality of service (QoS) requirement. Secondly, we investigate the sum rate maximization problem under power constraint using the weighted minimum mean squared error (WMMSE) method. Simulation results show that FAS outperforms FPA. Specifically, in the power minimization problem, FAS has a higher probability of achieving information rate constraint with less transmit power. In addition, the achieved sum rate of FAS is higher than that of FPA in the second problem.**

***Index Terms*—fluid antenna system, power allocation, transmit power minimization, sum rate maximization, WMMSE**

I. Introduction

In recent decades, the advent of multiple-input multiple-output (MIMO) technology has revolutionized wireless communications. This innovation exploits spatial diversity and multiplexing capability to improve the efficiency and performance of communication networks [1]. While MIMO enhances system performance without the need of additional bandwidth, it requires sophisticated signal processing to support multi-user communications. In addition, the massive connectivity provided by MIMO relies on a significant number of antennas and radio frequency (RF) chains at the base station (BS), which requires high hardware expense and power consumption [2], [3]. Although the fifth generation (5G) mobile communication allows the deployment of 64 or more antennas at a BS, the number of antennas feasible for a user equipment (UE) remains limited due to the confined space [4]. This limitation consequently restricts the performance of MIMO in mobile devices.

Recently, fluid antenna system (FAS) has opened new frontiers for the next generation of wireless communication by offering a unique and innovative approach to enable massive connectivity and enhance the performance of communication networks. Fluid antenna refers to any position-flexible antenna with the remarkable ability to dynamically adjust its characteristics, such as gain, radiation pattern, and operating frequency [5], [6]. The implementation of fluid antenna has been discussed in [7], including liquid-based antenna, reconfigurable pixel antenna, and movable antenna. By switching the antenna to select the strongest signal among preset positions (referred to as 'ports'), FAS achieves spatial degree of freedom (DoF) and diversity gain.

Many research efforts have already discussed the performance of FAS in the single-user case. In [8], the outage probability of FAS in the α-μ fading channels was analyzed. The closed-form analytical expressions of the average level crossing rate (LCR) of FAS were given in [9]. In [10], an analytical channel model considering eigenvalue decomposition was proposed, where the cross-correlation function of the ports is assumed to follow the Jake's model. The performance of FAS with the eigenvalue-based channel model in physical layer security was studied in [11], where a closed-form power allocation solution was provided for the wiretapping single-user scenario.

Fluid antenna is also ideal for multiple access as it can achieve interference immunity by switching the radiating element to where the interference signals experience a deep fade. This is referred to as fluid antenna multiple access (FAMA) [12], [13], where the interference is mitigated naturally using only one RF chain without complicated signal processing. The scheme in which the port of fluid antenna can be updated on a symbol-by-symbol basis is referred to as fast-FAMA (f-FAMA). The ability of fluid antenna to support multiple users was also investigated in [12] by studying the outage probability of the signal-to-interference ratio (SIR) and multiplexing gain of f-FAMA. In comparison, slow-FAMA (s-FAMA) is the approach that the fluid antenna only switches port when the fading channel changes, which can achieve multiplexing gain of 4 or larger [14].

The potential of combining FAS with other promising technologies has been considered in recent works [15]–[19]. In [15], Zheng et al. investigated the average block error rate (BLER) of the FAS-assisted non-orthogonal multiple access (NOMA) system. Compared with traditional full-duplex (FD) communication, the average sum rate of FD system can be greatly improved by cooperating with fluid antenna [16]. The outage probability and delay outage rate of reconfigurable intelligent surface (RIS)-aided FAS were derived in [17]. The

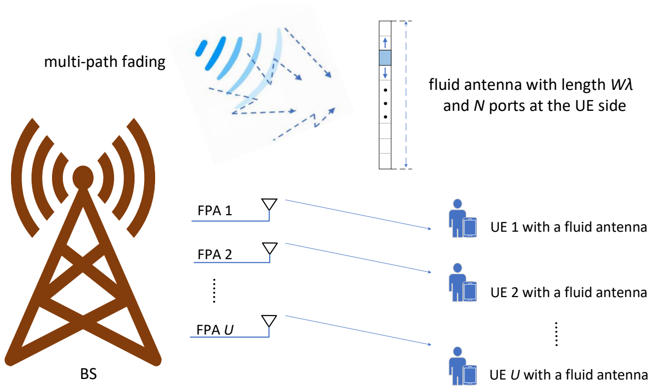

Fig. 1. A downlink multi-user FAS where the BS and the UEs are equipped with FPAs and fluid antennas, respectively.

application of FAS in terahertz band was studied in [18]. In addition, online learning was applied in [19] to select the optimal port for FAS.

In this paper, we investigate a downlink multi-user FAS, where the UEs and the BS are equipped with fluid antennas and fixed-position antennas (FPAs), respectively. Our objective is to optimize the transmit power of the BS to achieve better system performance. The performance of FPA is considered as a benchmark to show the benefits of FAS. The main contributions of this paper are summarized as follows:

- Firstly, we analyze the transmit power minimization problem for a downlink FAS-assisted communication scenario, where the information rate of each user needs to be larger than a threshold. We transform the constraint functions into linear form, and then use typical convex optimization tool to solve the problem. Simulation results show that FAS can achieve the rate constraints with much higher probability and lower transmit power compared to FPA.
- Then, we also consider the sum rate maximization problem with transmit power constraint at the BS. By introducing auxiliary functions, the proposed problem can be solved iteratively with a closed-form solution in each iteration. Simulation results depict that FAS achieves higher sum rate than FPA.

The remainder of this paper is organized as follows. Section II describes the system model and formulates two power allocation problems. In Section III, we solve the power minization and the sum rate maximization problems, respectively. Then, Section IV shows the simulation results of the proposed methods. Finally, Section V concludes this paper

II. System Model

A. Signal Model

As shown in Fig. 1, this paper considers a downlink multi-user FAS scenario, which consists of U UEs and a BS. The BS is equipped with U FPAs, and each antenna of the BS serves one UE. Each UE has a fluid antenna whose radiating element can be instantly switched to one of the N preset locations evenly distributed over a linear dimension of length $W\lambda$, where W denotes the normalized size of the fluid antenna and λ is the wavelength. The preset locations are referred to as ports, and the radiating element at each port is treated as an ideal point antenna. Without loss of generality (w.l.o.g.), we assume the information symbol intended for the u-th UE is transmitted by the u-th BS antenna. Then, the received signal at the k-th port of the u-th UE is given by

$$y_u^{(k)} = h_{u,u}^{(k)}\sqrt{p_u}s_u + \sum_{j\neq u}^{U} h_{j,u}^{(k)}\sqrt{p_j}s_j + n_u^{(k)}, \tag{1}$$

where $h_{j,u}^{(k)}$ represents the complex channel from the j-th BS antenna to the k-th port of the u-th UE, $s_j \sim \mathcal{CN}(0,1)$ and p_j denote the information symbol and transmit power for the j-th UE, and $n_u^{(k)} \sim \mathcal{CN}(0,\sigma_n^2)$ is the noise at the k-th port of the u-th UE.

B. Channel Model

Since the ports can be arbitrarily close to each other for small W and large N, $\forall u = 1,\dots,U$, the channels from the j-th BS antenna to different ports of the u-th UE, $h_{j,u}^{(k)}$ $\forall k$, are strongly correlated. The cross-correlation function of the ports is assumed to follow the Jake's model, and the covariance matrix $\mathbf{\Sigma}$ is employed to characterize the correlation of the channel gain vector $\boldsymbol{h}_{j,u} = \left[h_{j,u}^{(1)},\dots,h_{j,u}^{(N)}\right]^T$. Assume all the channels are independent and identically distributed (i.i.d.) and follow $\mathcal{CN}(0,\sigma^2)$, the (k,k')-th element of the covariance matrix is modeled as [10]

$$\mathbf{\Sigma}_{k,k'} = \sigma^2 J_0\left(\frac{2\pi\left(k-k'\right)W}{N-1}\right), \tag{2}$$

where $J_0(\cdot)$ denotes the zero-order Bessel function of the first kind. The eigen-decomposition of the covariance matrix $\mathbf{\Sigma}$ can be expressed as

$$\mathbf{\Sigma} = \boldsymbol{Q}\boldsymbol{\Lambda}\boldsymbol{Q}^H, \tag{3}$$

where the columns of $\boldsymbol{Q}$ are the eigenvectors of $\mathbf{\Sigma}$ and $\boldsymbol{\Lambda} = \text{diag}\left\{\lambda_1,\dots,\lambda_N\right\}$ is the diagonal matrix of eigenvalues. W.l.o.g., the eigenvalues are arranged in descending order, i.e., $\lambda_1 \geq \dots \geq \lambda_N$. Then, the channel gain vector is given by

$$\boldsymbol{h}_{j,u} = \boldsymbol{Q}\boldsymbol{\Lambda}^{\frac{1}{2}}\boldsymbol{x}_{j,u}, \tag{4}$$

where $\boldsymbol{x}_{j,u} = \left[x_{j,u}^{(1)},\dots,x_{j,u}^{(N)}\right]^T$ is a random vector with $x_{j,u}^{(k)} \sim \mathcal{CN}(0,1)$ $\forall k = 1,\dots,N$.

C. Problem Formulation

In this subsection, we aim to minimize the total transmit power of the BS and maximize the sum rate by power allocation, respectively. Before we proceed, we first assume that the k_u^*-th port is selected by the u-th UE to receive signal based on

$$k_u^* = \arg\max_k \frac{\left|h_{u,u}^{(k)}\right|^2}{\sum_{j\neq u}^U \left|h_{j,u}^{(k)}\right|^2}. \tag{5}$$

Then, the received signal of the u-th UE is

$$y_u = h_{u,u}\sqrt{p_u}s_u + \sum_{j\neq u}^U h_{j,u}\sqrt{p_j}s_j + n_u, \tag{6}$$

where $h_{j,u} \triangleq h_{j,u}^{(k_u^*)}$ and $n_u \triangleq n_u^{(k_u^*)}$. The signal to interference plus noise ratio (SINR) of the u-th UE is written as

$$\eta_u = \frac{p_u \left|h_{u,u}\right|^2}{\sum_{j\neq u}^U p_j \left|h_{j,u}\right|^2 + \sigma_n^2}. \tag{7}$$

The information rate of the u-th UE is thus expressed as

$$R_u = \log\left(1+\eta_u\right). \tag{8}$$

In this paper, we consider two optimization problems, i.e., total power minimization and sum rate maximization.

1) Total Transmit Power Minimization: Our first objective is to minimize the total transmit power of the BS while guaranteeing the transmission quality of all the UEs. The problem is formulated as

$$\begin{aligned} \min_{p_{\mathcal{U}}} \quad & \sum_{u=1}^U p_u \\ \text{s.t.} \quad & R_u \geq \gamma_u,\ \forall u \in \mathcal{U}, \\ & p_u \geq 0,\ \forall u \in \mathcal{U}, \end{aligned} \tag{9}$$

where $\mathcal{U} = \{1, \cdots, U\}$ denotes the user index and γ_u is the data rate threshold of the u-th UE .

2) Sum Rate Maximization: Secondly, we aim to maximize the sum rate of the system under power constraint, i.e.,

$$\begin{aligned} \max_{p_{\mathcal{U}}} \quad & \sum_{u=1}^U R_u \\ \text{s.t.} \quad & \sum_{u=1}^U p_u \leq P, \\ & p_u \geq 0,\ \forall u \in \mathcal{U}, \end{aligned} \tag{10}$$

where P is the maximum transmit power of the BS.

III. Problem Solution

In this section, we solve problems (9) and (10), respectively.

A. Total Transmit Power Minimization

Dropping the $\log(\cdot)$ operation, problem (9) is equivalent to

$$\begin{aligned} \min_{p_{\mathcal{U}}} \quad & \sum_{u=1}^U p_u \\ \text{s.t.} \quad & \frac{1}{\epsilon_u} p_u \left|h_{u,u}\right|^2 - \sum_{j\neq u}^U p_j \left|h_{j,u}\right|^2 - \sigma_n^2 \geq 0,\ \forall u \in \mathcal{U}, \\ & p_u \geq 0,\ \forall u \in \mathcal{U}, \end{aligned} \tag{11}$$

where $\epsilon_u = 2^{\gamma_u} - 1$. Since the objective function and all constraint functions are linear, (11) is a linear programming problem, and can thus be solved using CVX.

B. Sum Rate Maximization

As problem (10) is non-convex and difficult to solve, we use the weighted minimum mean squared error (WMMSE) method [20]. Assume that the minimum mean squared error (MMSE) receiver is applied at the UEs to estimate the desired symbol. At the u-th UE, the mean squared error (MSE) is given by

$$\begin{aligned} & MSE_u \\ =& \mathrm{E}\left[\left|f_u^H y_u - s_u\right|^2\right] \\ =& \left|f_u\right|^2 \left(\sum_{j=1}^U \left|h_{j,u}\right|^2 p_j + \sigma_n^2\right) - f_u h_{u,u}^H \sqrt{p_u} - f_u^H h_{u,u}\sqrt{p_u} + 1, \end{aligned} \tag{12}$$

where f_u is the single-tap linear scaling at the u-th UE. The minimum value of MSE_u is obtained at

$$f_u^* = \frac{h_{u,u}\sqrt{p_u}}{\sum_{j=1}^U \left|h_{j,u}\right|^2 p_j + \sigma_n^2}. \tag{13}$$

Then, the minimum value of MSE_u is

$$\begin{aligned} MMSE_u &= MSE_u\left(f_u^*\right) \\ &= 1 - \frac{\left|h_{u,u}\right|^2 p_u}{\sum_{j=1}^U \left|h_{j,u}\right|^2 p_j + \sigma_n^2} \\ &= \frac{\sum_{j\neq u}^U \left|h_{j,u}\right|^2 p_j + \sigma_n^2}{\sum_{j=1}^U \left|h_{j,u}\right|^2 p_j + \sigma_n^2} \\ &= \frac{1}{1+\eta_u}. \end{aligned} \tag{14}$$

Problem (10) can thus be reformulated as

$$\begin{aligned} \min_{p_{\mathcal{U}}, f_{\mathcal{U}}} \quad & \sum_{u=1}^U \ln\left(MSE_u\right) \\ \text{s.t.} \quad & \sum_{u=1}^U p_u \leq P, \\ & p_u \geq 0,\ \forall u \in \mathcal{U}. \end{aligned} \tag{15}$$

As problem (15) is still non-convex, we iteratively optimize $p_{\mathcal{U}}$ and $f_{\mathcal{U}}$. Firstly, for fixed $p_{\mathcal{U}}$, the solution of (15) is $f_{\mathcal{U}}^* = \{f_1^*, \cdots, f_U^*\}$, where $f_u^*\ \forall u \in \mathcal{U}$ is given in (13). However, for fixed $f_{\mathcal{U}}$, problem (15) becomes

$$\begin{aligned} \min_{p_{\mathcal{U}}} \quad & \sum_{u=1}^U \ln\left(MSE_u\right) \\ \text{s.t.} \quad & \sum_{u=1}^U p_u \leq P, \\ & p_u \geq 0,\ \forall u \in \mathcal{U}, \end{aligned} \tag{16}$$

which is non-convex and intractable. To remove the $\ln(\cdot)$ operation, we introduce auxiliary functions $G_{\mathcal{U}}$, where

$$G_u\left(r_u\right) = e^{r_u - 1} MSE_u - r_u,\ \forall u \in \mathcal{U}. \tag{17}$$

The first order derivative of $G_u\left(r_u\right)$ over r_u is given by

$$\frac{\partial G_u\left(r_u\right)}{\partial r_u} = e^{r_u - 1} MSE_u - 1. \tag{18}$$

Since the second order derivative of $G_u\left(r_u\right)$ is non-negative, its minimum value $G_u\left(r_u^*\right) = \ln\left(MSE_u\right)$ is obtained when $\frac{\partial G_u(r_u)}{\partial r_u} = 0$, where

$$r_u^* = 1 + \ln\left(\frac{1}{MSE_u}\right). \tag{19}$$

Problem (16) is thus equivalent to

$$\begin{aligned} \min_{p_{\mathcal{U}}} \quad & \sum_{u=1}^{U} G_u\left(r_u^*\right) = e^{r_u^* - 1} MSE_u - r_u^* \\ \text{s.t.} \quad & \sum_{u=1}^{U} p_u \le P, \\ & p_u \ge 0,\ \forall u \in \mathcal{U}. \end{aligned} \tag{20}$$

Based on (12), the objective function of problem (20) after dropping constants is equivalent to

$$\begin{aligned} & \sum_{u=1}^{U} p_u \left(\sum_{j=1}^{U} e^{r_j^* - 1} \left|f_j\right|^2 \left|h_{u,j}\right|^2 \right) \\ & - \sqrt{p_u} e^{r_u^* - 1} \left(f_u h_{u,u}^H + f_u^H h_{u,u} \right) \\ = & \sum_{u=1}^{U} q_u^2 a_u - q_u b_u, \end{aligned} \tag{21}$$

where $q_u = \sqrt{p_u}$, $a_u = \sum_{j=1}^{U} e^{r_j^* - 1} \left|f_j\right|^2 \left|h_{u,j}\right|^2$ and $b_u = e^{r_u^* - 1}\left(f_u h_{u,u}^H + f_u^H h_{u,u}\right)$. Then, problem (20) can be rewritten in matrix form as

$$\begin{aligned} \min_{\boldsymbol{q}} \quad & z\left(\boldsymbol{q}\right) = \boldsymbol{q}^T \boldsymbol{A} \boldsymbol{q} - \boldsymbol{b} \boldsymbol{q} \\ \text{s.t.} \quad & \boldsymbol{q}^T \boldsymbol{q} - P \le 0, \\ & q_u \ge 0,\ \forall u \in \mathcal{U}, \end{aligned} \tag{22}$$

where $\boldsymbol{q} = \left[q_1, \ldots, q_U\right]^T$, $\boldsymbol{A} = \operatorname{diag}\left\{a_1, \ldots, a_U\right\}$, $\boldsymbol{b} = \left[b_1, \ldots, b_U\right]$. The first order derivative of $z\left(\boldsymbol{q}\right)$ is given by

$$\frac{\partial z\left(\boldsymbol{q}\right)}{\partial \boldsymbol{q}} = 2\boldsymbol{A}\boldsymbol{q} - \boldsymbol{b}^T, \tag{23}$$

which is $\mathbf{0}$ at

$$\boldsymbol{q}' = \frac{1}{2}\boldsymbol{A}^{-1}\boldsymbol{b}^T. \tag{24}$$

Since the Hessian matrix of $z\left(\boldsymbol{q}\right)$ is equal to $2\boldsymbol{A}$ and thus positive-definite, the minimum value of the objective function of problem (22) is $z\left(\boldsymbol{q}'\right)$. Since $a_u > 0$ and $b_u \ge 0\ \forall u \in \mathcal{U}$, we have ${q'}_u \ge 0$, the second constraint of (22) is thus satisfied. If ${\boldsymbol{q}'}^T \boldsymbol{q}' - P \le 0$, then $\boldsymbol{q}'$ is the optimal solution of problem (22).

Otherwise, i.e., ${\boldsymbol{q}'}^T \boldsymbol{q}' - P > 0$, the optimal value of $\boldsymbol{q}$ is on the boundary of the feasible set and the direction of the negative gradient is the same as the outward pointing normal. Therefore, the optimal solution $\boldsymbol{q}^*$ of problem (22) satisfies ${\boldsymbol{q}^*}^T \boldsymbol{q}^* - P = 0$ and $\frac{\partial z(\boldsymbol{q})}{\partial \boldsymbol{q}^*} = -\lambda \boldsymbol{q}^*$ for some $\lambda > 0$. From (23), we have $2\boldsymbol{A}\boldsymbol{q}^* - \boldsymbol{b}^T = -\lambda \boldsymbol{q}^*$ for some $\lambda > 0$. Therefore, we derive

$$\boldsymbol{q}^* = \left(2\boldsymbol{A} + \lambda \boldsymbol{I}\right)^{-1} \boldsymbol{b}^T. \tag{25}$$

To find λ, we define

$$g(\lambda) = {\boldsymbol{q}^*}^T \boldsymbol{q}^* = \sum_{u=1}^{U} \frac{b_u^2}{(2a_u + \lambda)^2}. \tag{26}$$

The first order derivative of $g(\lambda)$ is given by

$$\frac{\partial g(\lambda)}{\partial \lambda} = \sum_{u=1}^{U} \frac{-2b_u^2}{(2a_u + \lambda)^3}. \tag{27}$$

Since $\lambda > 0$ and $a_u > 0\ \forall u \in \mathcal{U}$, we know that $\frac{\partial g(\lambda)}{\partial \lambda} < 0$. Therefore, $g(\lambda)$ monotonically decreases to 0 as λ goes to infinity. When $\lambda = 0$, we have $g(0) = \sum_{u=1}^{U} \frac{b_u^2}{(2a_u)^2} = {\boldsymbol{q}'}^T \boldsymbol{q}' > P$. Since equation $g(\lambda) = {\boldsymbol{q}^*}^T \boldsymbol{q}^* = P$ has exactly one positive solution λ^*, $\boldsymbol{q}^*$ can be obtained by searching λ^*. We use bisection search to find the optimal λ and $\boldsymbol{q}$, and then obtain the solution of problem (10) as $p_u = q_u^2,\ \forall u \in \mathcal{U}$. The main steps of solving (10) are summarized in Algorithm 1.

Algorithm 1 Solution for Problem (10)

1: Initialize $p_{\mathcal{U}}$.
2: **repeat**
3: Update $f_{\mathcal{U}}$ based on (13).
4: Update $r_{\mathcal{U}}$ based on (19) and (12).
5: Calculate $\boldsymbol{q}'$ based on (24).
6: Let $\boldsymbol{q} = \boldsymbol{q}'$ if ${\boldsymbol{q}'}^T \boldsymbol{q}' - P \le 0$. Otherwise, search λ^* which satisfies $g(\lambda^*) = P$, and then update $\boldsymbol{q}$ based on (25).
7: **until** convergence
8: Let $p_u = q_u^2,\ \forall u \in \mathcal{U}$ be the solution of problem (10).

IV. Simultion Results

In this section, we demonstrate the performance of the proposed algorithms using Monte Carlo simulation. The noise power is set to be 1 Watt, and the maximum transmit power for problem (10) is $P = 100 * U$ Watt.

In Fig. 2, we investigate if FAS can help minimize the transmit power while satisfying the information rate constraints of problem (9). W.l.o.g., we set $\gamma_u = \gamma = 1,\ \forall u \in \mathcal{U}$. We define an outage event when there is no solution for problem (9). From the first figure, we can observe that the rate limits are always guaranteed by fluid antenna with 10 ports while outage events happen in 50% and 90% of channel realizations for FPA in 2 and 3 UEs cases, respectively. In comparison, the outage probability of fluid antenna with 2

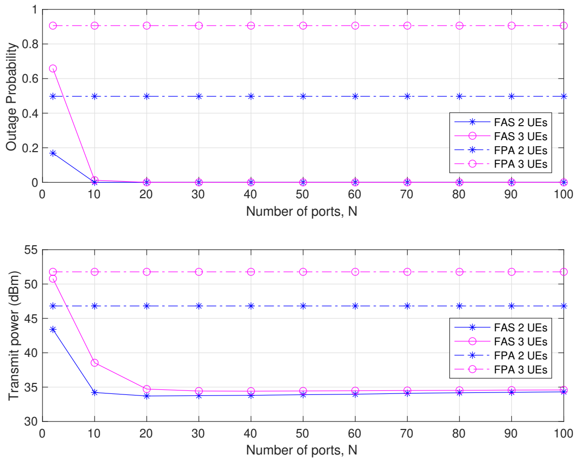

Fig. 2. Outage probability and transmit power of problem (9) versus the number of ports of fluid antenna with $W = 5$ and $\gamma = 1$.

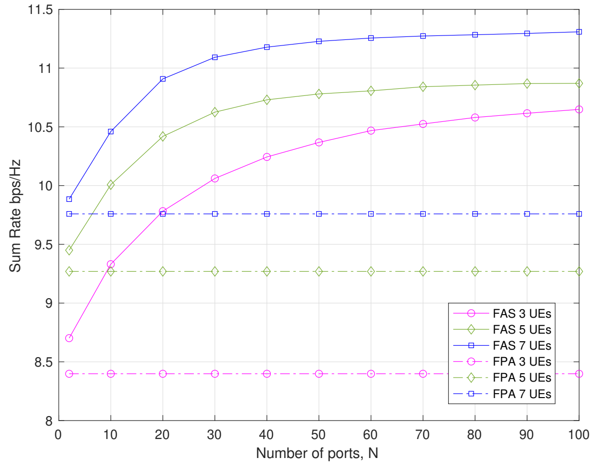

Fig. 4. Sum rate of problem (10) versus the number of ports of fluid antenna with $W = 5$.

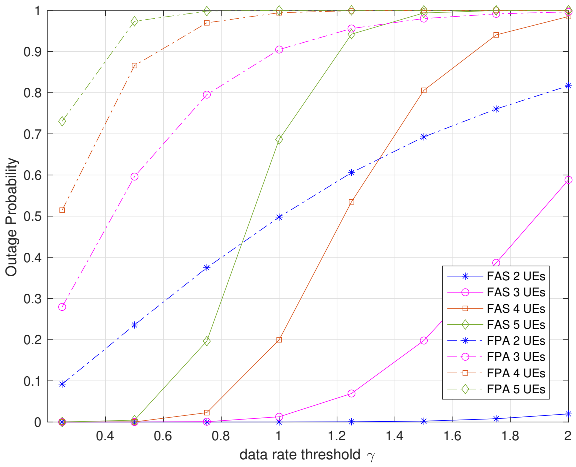

Fig. 3. Outage probability of problem (9) versus data rate threshold with $W = 5$ and $N = 10$.

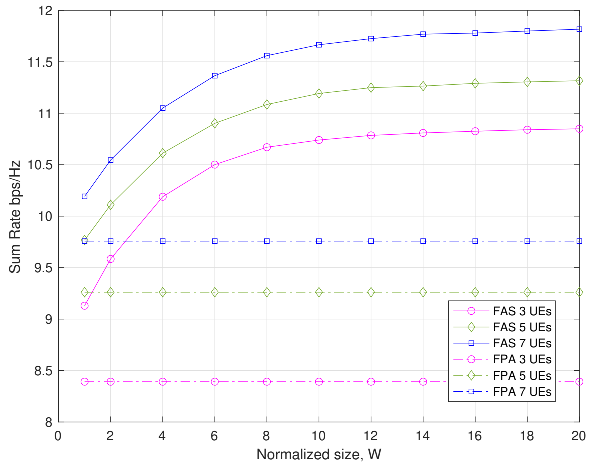

Fig. 5. Sum rate of problem (10) versus normalized size of fluid antenna with $N = 50$.

ports in 3 UEs case is 65%, and it reduces to 0 as the number of ports of fluid antenna increases. The second figure in Fig. 2 demonstrates how the required transmit power changes with the number of ports of fluid antenna. As expected, by switching fluid antenna among more ports, the BS needs less power to guarantee the transmission. Specifically, in 3 UEs case, the transmit power reduces from 51 dBm to 35 dBm as the the number of ports increases. The required transmit power of fluid antenna with 20 ports is 17 dB less than that of FPA when there are 3 UEs in the system.

Fig. 3 depicts the outage performance of problem (9) with different data rate thresholds. As it is more difficult to reach the higher information rate, the outage probability increases with γ. When the number of UEs in the system increases, the power of interference signals received by each UE increases, which makes it more difficult to reach the rate constraints. From the figure, we can see that in 2 UEs case, FAS can always satisfy the rate requirement even with large γ while the outage probability of FPA increases to more than 80%.

In Fig. 4, we analyze how the achieved sum rate of problem (10) changes with the port number of fluid antenna. As expected, the sum rate firstly increases with the number of ports due to the introduced diversity. Since the ports become highly correlated for a given antenna size with large N, increasing the number of ports further cannot bring more performance gain. Therefore, the sum rate saturates at some large N. The performance of FAS saturates faster when there are more UEs in the system. This is because the increasing number of UEs results in more interference in the system, which limits the performance gain by changing the antenna position. Compared to FPA, the sum rate of fluid antenna with 100 ports is increased by 26% in 3 UEs case.

Fig. 5 shows the relationship between sum rate and the normalized size of fluid antenna. From the figure, we can observe that the sum rate initially increases with the size of fluid antenna due to the introduced degree of freedom. The performance then reaches the peak since the resolution reduces as the antenna size increases. For a given number of UEs, FAS outperforms FPA in terms of sum rate. In particular, the sum rate of FAS in 7 UEs case increases from 10.2 bps/Hz to 11.8 bps/Hz as W increases from 2 to 20. In comparison, the sum rate of FPA is 9.75 bps/Hz when there are 7 UEs in the system.

V. Conclusion

In this paper, we considered two power allocation problems for FAS. We first minimized the transmit power of the BS with information rate constraint for each UE. By transforming the constraint functions into linear form, we solved the problem globally using linear programming solver. The results of FAS were compared with those of FPA to show the advantages of switching antenna within a given region. In particular, FAS has a higher probability and requires less power to reach the rate limits. After that, we maximized the system sum rate when the total transmit power is restricted. With introduced auxiliary functions, a closed-form solution was derived using WMMSE method. Simulation results showed that FAS can achieve higher sum rate compared to FPA.

References

[1] Z. H. Shaik, E. Björnson, and E. G. Larsson, "Cell-free massive MIMO with radio stripes and sequential uplink processing," in *Proc. IEEE Int. Conf. Commun. Workshops (ICC Workshops)*, Dublin, Ireland, Jun. 2020, pp. 1–6.

[2] A. Kaushik, C. Masouros, and F. Liu, "Hardware efficient joint radar-communications with hybrid precoding and RF chain optimization," in *Proc. IEEE Int. Conf. Commun. (ICC)*, Montreal, QC, Canada, Jun. 2021, pp. 1–6.

[3] H. Q. Ngo, E. G. Larsson, and T. L. Marzetta, "Energy and spectral efficiency of very large multiuser MIMO systems," *IEEE Trans. Commun.*, vol. 61, no. 4, pp. 1436–1449, Apr. 2013.

[4] H. Asplund and *et al.*, *Advanced antenna systems for 5G network deployments: bridging the gap between theory and practice*. Academic Press, 2020.

[5] K.-K. Wong, A. Shojaeifard, K.-F. Tong, and Y. Zhang, "Fluid antenna systems," *IEEE Trans. Wireless Commun.*, vol. 20, no. 3, pp. 1950–1962, Mar. 2020.

[6] H. Xu, G. Zhou, K.-K. Wong, W. K. New, C. Wang, C.-B. Chae, R. Murch, S. Jin, and Y. Zhang, "Channel estimation for FAS-assisted multiuser mmWave systems," *IEEE Commun. Lett.*, vol. 28, no. 3, pp. 632–636, Mar. 2024.

[7] L. Zhu and K.-K. Wong, "Historical review of fluid antenna and movable antenna," *arXiv preprint, arXiv:2401.02362v2*, 2024.

[8] P. D. Alvim, H. S. Silva, F. O. Barcelos, P. R. de Moura, U. S. Dias, O. S. Badarneh, and R. A. A. de Souza, "On the performance of fluid antenna systems under α-μ fading channels," *IEEE Wireless Commun. Lett.*, vol. 13, no. 1, pp. 108–112, Jan. 2024.

[9] P. Mukherjee, C. Psomas, and I. Krikidis, "On the level crossing rate of fluid antenna systems," in *Proc. IEEE 23rd Int. Workshop Sig. Process. Advances Wireless Commun. (SPAWC)*, Jul. 2022, Oulu, Finland.

[10] M. Khammassi, A. Kammoun, and M.-S. Alouini, "A new analytical approximation of the fluid antenna system channel," *IEEE Trans. Wireless Commun.*, vol. 22, no. 12, pp. 8843–8858, Dec. 2023.

[11] B. Tang, H. Xu, K.-K. Wong, K.-F. Tong, Y. Zhang, and C.-B. Chae, "Fluid antenna enabling secret communications," *IEEE Commun. Lett.*, vol. 27, no. 6, pp. 1491–1495, Jun. 2023.

[12] K.-K. Wong and K.-F. Tong, "Fluid antenna multiple access," *IEEE Trans. Wireless Commun.*, vol. 21, no. 7, pp. 4801–4815, Jul. 2022.

[13] H. Xu, K.-K. Wong, W. K. New, K.-F. Tong, Y. Zhang, and C.-B. Chae, "Revisiting outage probability analysis for two-user fluid antenna multiple access system," *IEEE Trans. Wireless Commun.*, early access, 2024.

[14] K.-K. Wong, D. Morales-Jimenez, K.-F. Tong, and C.-B. Chae, "Slow fluid antenna multiple access," *IEEE Trans. Commun.*, May 2023.

[15] J. Zheng, T. Wu, X. Lai, C. Pan, M. Elkashlan, and K.-K. Wong, "FAS-assisted NOMA short-packet communication systems," *IEEE Trans. Veh. Technol.*, early access, 2024.

[16] C. Skouroumounis and I. Krikidis, "Fluid antenna-aided full duplex communications: A macroscopic point-of-view," *IEEE J. Sel. Areas Commun.*, vol. 41, no. 9, pp. 2879–2892, Sep. 2023.

[17] F. R. Ghadi, K.-K. Wong, W. K. New, H. Xu, R. Murch, and Y. Zhang, "On performance of RIS-aided fluid antenna systems," *arXiv preprint arXiv:2402.16116*, 2024.

[18] L. Tlebaldiyeva, S. Arzykulov, K. M. Rabie, X. Li, and G. Nauryzbayev, "Outage performance of fluid antenna system (FAS)-aided terahertz communication networks," in *Proc. IEEE Int. Conf. Commun. (ICC)*, Rome, Italy, May 2023.

[19] J. Zou, S. Sun, and C. Wang, "Online learning-induced port selection for fluid antenna in dynamic channel environment," *IEEE Wireless Commun. Lett.*, vol. 13, no. 2, pp. 313–317, Feb. 2024.

[20] H. Xu, G. Caire, W. Xu, and M. Chen, "Weighted sum secrecy rate maximization for D2D underlaid cellular networks," *IEEE Trans. Commun.*, vol. 68, no. 1, pp. 349–362, Jan. 2020.